UDC 551.515.5:551.509.313(729.61)"1966.08.09–11"

DIAGNOSTIC STUDY OF A TROPICAL DISTURBANCE

CARL O. ERICKSON

National Environmental Satellite Service, NOAA, Washington, D.C.

ABSTRACT

An area of disturbed weather over the Bahamas is studied in detail for the 3-day period, Aug. 9–11, 1966. The coupling of an upper level cold-core cyclone with an approaching low-level wave was largely responsible for the considerable increase in cloudiness and weather observed on August 9 and 10.

Warm anomalies in the lower stratosphere were even larger than the cold anomalies of the upper troposphere, strongly suggesting the existence of large-scale vertical motions at both levels.

Results from a diagnostic numerical model show that the Laplacian of thermal advection was the single most important forcing function contributing to tropospheric vertical motion. Agreement between observed cloudiness and calculated vertical motion was generally good.

1. INTRODUCTION

On Aug. 9 and 10, 1966, a dramatic increase in cloudiness and weather was observed over the Bahama Islands in the vicinity of an upper tropospheric cold Low. The reasons for the increase were not immediately apparent. Low-level flow was only weakly perturbed, and the upper level cyclone actually diminished in intensity from August 9 onward. Although the weather was not severe and the disturbance never threatened to produce a tropical storm, it did present an important forecasting problem for the Bahamas and south Florida.

This study was undertaken in an effort to achieve a better understanding of the reasons for the cloud development. This development was observed in the APT (automatic picture transmission) satellite photographs received operationally. Additional favorable factors were that the disturbance was located over an area of relatively good conventional data, and a numerical diagnostic model designed by Krishnamurti (1968) was available. The initial course of the investigation, then, was to apply Krishnamurti's diagnostic model to this case in which considerable cloud enhancement as seen by satellite occurred and to determine the most important influences in the development. Detailed hand analyses were performed, and numerical results were obtained for Aug. 9–11, 1966.

The numerical results include a number of parameters, and their complete analysis is beyond the scope of this report. The objective of this study, which was to determine the causes of the observed cloud enhancement, was best served by examination of the partitioned analyses of vertical motion (ω). The main result of significance, and the one that is emphasized in this report, is that the Laplacian of thermal advection was the dominant factor in the calculated ω pattern.

As this investigation progressed, it became increasingly apparent that there was a linkage between the slow-moving upper level cyclone over the Bahamas and a more rapidly moving low-level wave approaching the area from the east. The linkage involved a moisture influx from the low-level wave into the middle and upper levels of the cold Low, but the interaction did *not* enhance the horizontal circulation at either level. Because this evolving relationship between upper level cyclone and lower level wave was a vital contributor to the observed weather, it is presented as an integral part of the synoptic discussion.

It is, of course, well known that large changes in local cloudiness and weather, such as occurred in this case, can result from subtle changes in the conditionally unstable tropical atmosphere; and it has been indicated that linkage between weather systems of the upper and lower troposphere may be a mechanism for such changes (Krishnamurti and Baumhefner 1966, Frank 1969, Riehl 1954, Simpson et al. 1967). However, because of general data problems over the Tropics, the interaction between upper and lower levels has not often been well documented. Therefore, study of this case provides an excellent opportunity for observing details of the mechanism of such interaction.

2. ANALYSIS AREAS AND DATA SOURCES

All available surface, rawinsonde, commercial aircraft, and satellite data were used in the preparation of hand analyses at constant-pressure levels (1000, 850, 700, 500, 300, 200, and 100 mb). The analyses of wind and temperature (to 200 mb) and moisture (to 500 mb) in turn provided input to the numerical diagnostic model designed by Krishnamurti (1968). Figure 1 (entire area) shows the region of the constant-pressure analyses. The smaller rectangle, 12°–33°N, 55°–94°W, represents the area of numerical calculations. The grid-point interval was 1½° of latitude and longitude for both input and output (sample in upper right of area).[1]

The location of the vertical cross sections—a rhumb line through Miami, Fla, and Raizet, Guadeloupe—was chosen so as to pass nearly through the 200-mb Low center on August 9, 10, and 11. A number of rawinsonde stations lie near the cross section line, facilitating reasonably accurate analyses. The shaded area extending 150 n.mi. on either side of the line is the region of accompanying surface data.

[1] In figure 1, the eastward extension of the numerical area to 46°W (enclosed by heavy dashed lines) represents the additional output necessary to establish cyclical continuity with the western boundary. See Krishnamurti (1968) for details.

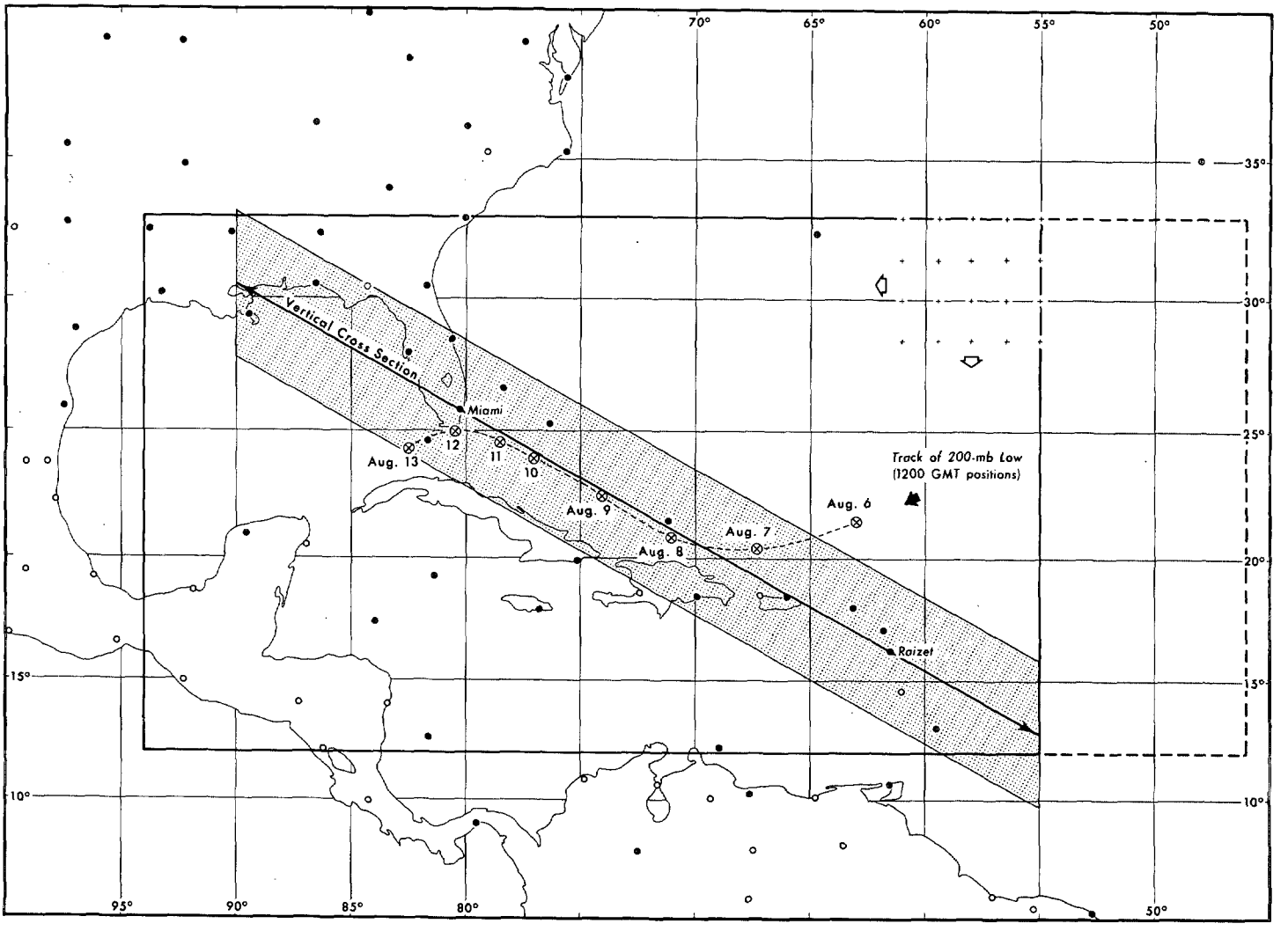

FIGURE 1.—Map of the analysis areas, location of the vertical cross sections, and track of the 200-mb Low center. Also shown are the locations of rawinsonde stations (dots) and pibal stations (open circles) reporting at 1200 GMT.

Nearly all the rawinsonde data were obtained either from the checked data of the Northern Hemisphere Data Tabulations at the National Environmental Satellite Service or from copies of original records at the Environmental Data Service, National Weather Records Center, Asheville, N.C. Most soundings near the cross sections were recomputed, and conservative adjustments to reported temperatures and heights made where necessary (after the method of Hawson and Caton 1961 as adapted by Carlson 1967). While these adjustments were mostly minor, there were several soundings with rather large errors.

An additional adjustment was applied to all tropospheric temperature data (except those on the time sections) in the form of vertical smoothing over an interval of 100 mb, using the mean Caribbean August atmosphere (Jordan 1957) as a base. A three-point binomial smoother was used. Because such smoothing reduces individual deviations while leaving the mean temperature of deep air columns unchanged, the corresponding height adjustments are negligible.

A number of pibal stations exist within the analysis area of figure 1, but relatively few upper wind data were obtained from those stations.

3. SATELLITE AND SURFACE CLOUD OBSERVATIONS

Figure 2 shows cloud photographs of the Bahamas and surrounding areas for Aug. 8–11, 1966. Unfortunately, satellite coverage other than APT was limited during that period, and these ESSA 2 photomosaics (reproduced from facsimile copy) provide the best overall view. Nearly all of the individual photographs were taken within 2 hr of the 1200 GMT synoptic hour.

Most striking is the large increase in cloudiness associated with the 200-mb Low during August 8–10. On August 8 (fig. 2a), it is seen that only scattered cumuliform clouds existed in the area of the Low. The island of Hispaniola, partly outlined by specular reflection, is clearly visible. By August 9, a dense mass of convective and multilayer cloud had appeared near 70°W—just east of the 200-mb Low center. (Specular reflection again is seen over the largely cloud-free waters surrounding Jamaica and eastern Cuba.) By August 10, a further increase in cloudiness had occurred, spreading to all quadrants of the Low. Overall cloudiness showed a slight decrease by August 11, but dense broken masses persisted through that day and for 2 or 3 days thereafter.

Surface observations of sky cover, plotted in figure 3

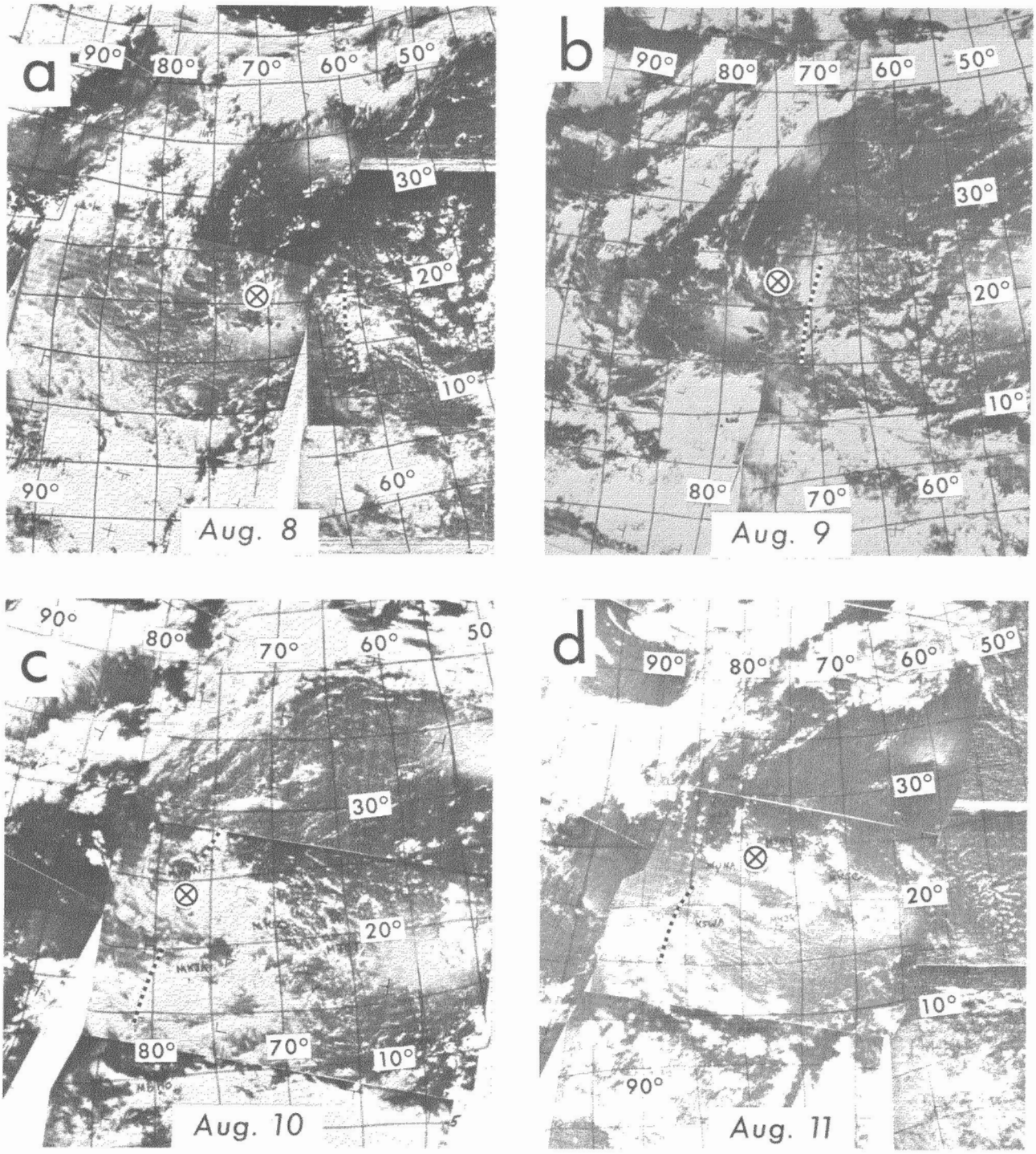

FIGURE 2.—ESSA 2 cloud photographs for Aug. 8–11, 1966. Location of the 200-mb Low center at 1200 GMT is indicated by a cross within a circle. The position of the surface wave at the same time is shown by a dotted line.

also provide some indication of the areal cloud distributions on August 9, 10, and 11. However, the dramatic satellite-observed increase over the Bahamas on August 10, seen in figure 2c, is not nearly as obvious in these plotted surface observations for the same day in figure 3b. (This probably reflects the long-noted inadequacies of both point observations and the surface synoptic code as applied to tropical cloud systems.) Direct comparison of figures 2 and 3 is aided by noting the positions of the 200-mb Low and the surface wave. Those features appear on both figures.

Figures 2 and 3 show that the increase in cloudiness (and weather) in the vicinity of the upper level Low during August 9 and 10 occurred as the low-level wave approached and moved under the upper level Low. This is discussed in more detail in the next section.

4. METEOROLOGICAL ANALYSES FOR AUGUST 9–11

SYNOPTIC SITUATION AT 1200 GMT ON AUGUST 9

Some features of the vertical structure of the troposphere at 1200 GMT on August 9 may be seen in the

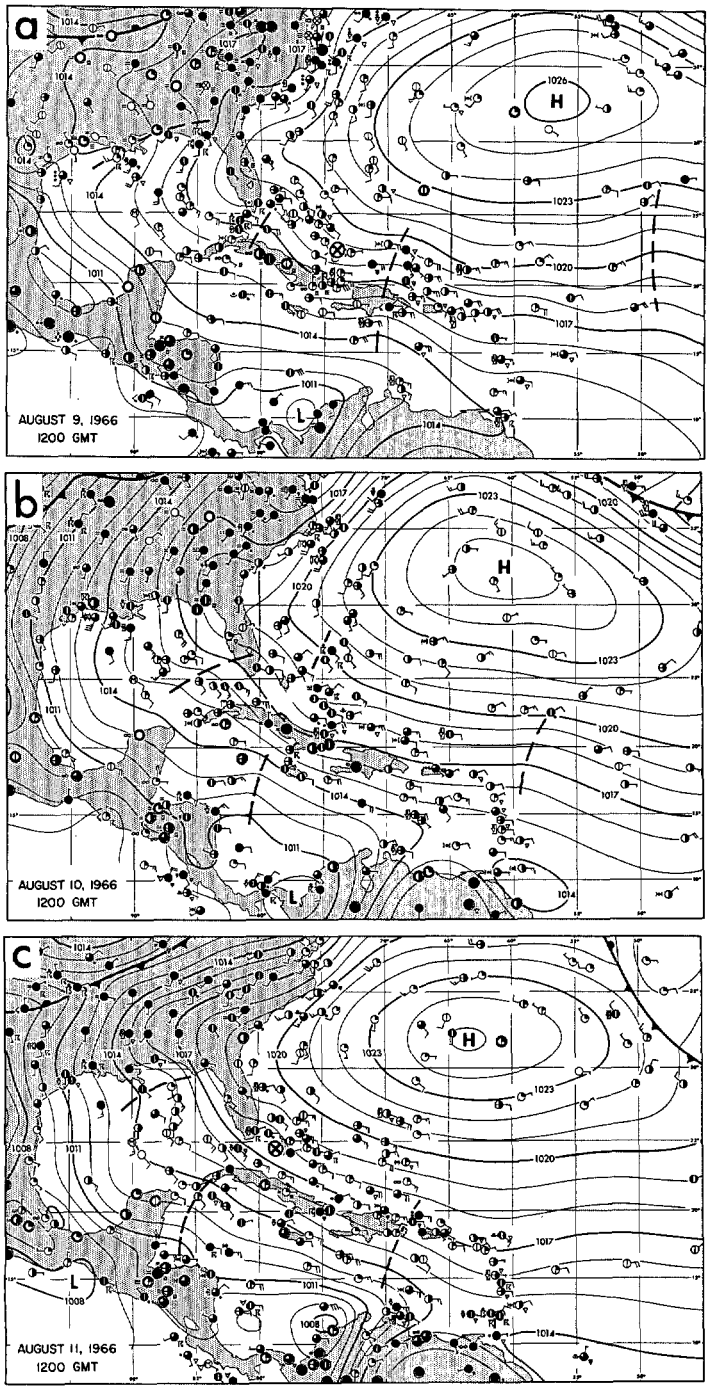

FIGURE 3.—The 1200 GMT surface charts for Aug. 9–11, 1966. The abbreviated plotted data include sky cover, wind, and present and past weather. The location of the 200-mb Low center is denoted by a cross within a circle.

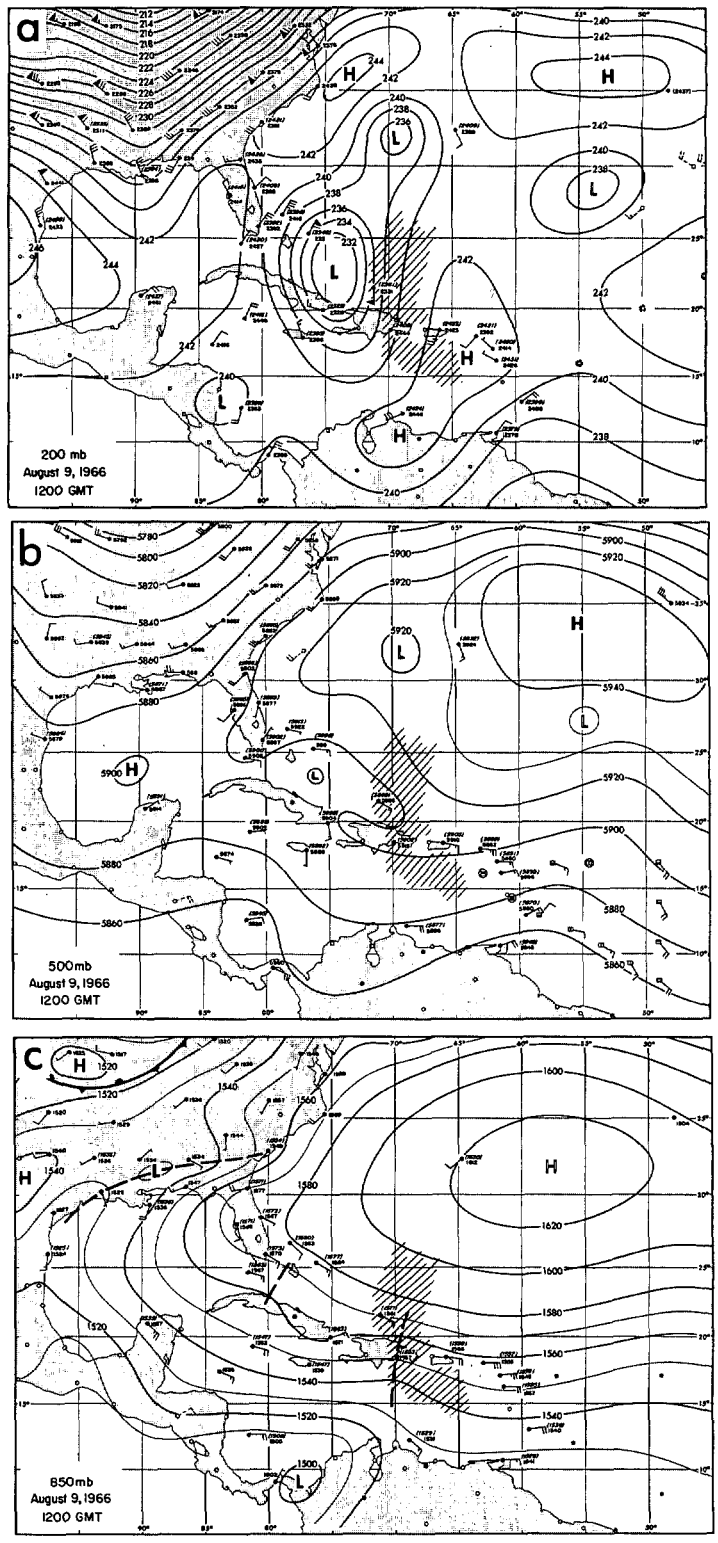

FIGURE 4.—The 200-, 500-, and 850-mb contours (gpm) for 1200 GMT on August 9. The recomputed height values at some individual stations (slanted numbers in parentheses) are plotted above the reported values. The hatched area is a region of heavy cloudiness.

constant-pressure analyses of figures 4 and 5 and the vertical cross section of figure 6. The axis of the upper level cyclonic system over the Bahamas sloped eastward, and the circulation increased with altitude, achieving maximum intensity near 200 mb. The cold-core nature of the cyclone below that level is revealed by the isotherms at 300 and 700 mb (fig. 5) and by the large area of negative temperature anomaly (fig. 6). Above the 200-mb Low center (fig. 6), a strong reversal occurred, with relatively high temperatures in the layer 150–100 mb and a rapid weakening of the cyclone upward. The tropopause was almost nonexistent—a significant point discussed later.

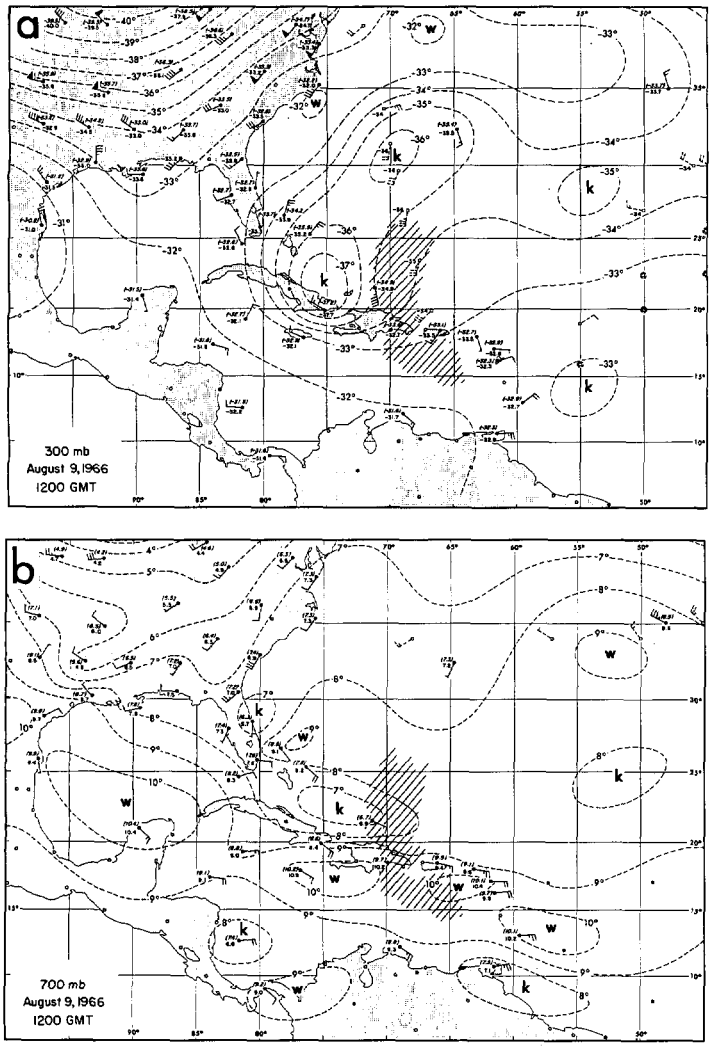

FIGURE 5.—The 300- and 700-mb isotherms (1°C interval) for 1200 GMT on August 9. Both the reported temperatures (lower figures) and the smoothed recalculated temperatures (upper slanted figures in parentheses) are plotted at individual stations. The hatched area is a region of heavy cloudiness.

At the surface at the same time (fig. 3a), the only reflection of the upper level cyclone was the very weak trough just southeast of the Florida Peninsula together with the scattered showers and thunderstorms in that area (see also the surface data in fig. 6). The weak trough near 70°W is the "approaching low-level wave" previously mentioned. Although well marked by a band of overcast and showers at 1200 GMT on August 9, this wave, as a perturbation in the wind field, was of very limited vertical extent at that time (fig. 6). Clearly, it was not directly connected to the upper level cold Low.

HISTORY OF LOW-LEVEL WAVE

Figure 7 shows the relative positions of the 200-mb Low center and the surface wave on August 8–11 as well as the successive passages of the wave at Raizet, Guadeloupe (16°N, 61.5°W), San Juan, Puerto Rico (18.5°N, 66°W), and Turks Island (21.5°N, 71°W). The perturbation weakened markedly as it proceeded west-northwestward. Continuity is well maintained, however, by the band of heavy clouds and showers that passed all three stations (as well as by the surface analyses at synoptic hours). These indicate a wave speed of 15–20 kt.

A surge of moisture accompanied the wave. This is seen in figure 8 during wave passage at San Juan. A similar and even more pronounced moisture surge occurred earlier at Raizet (not shown).

Westward progress of the low-level wave also is discernible in the cloud photographs of figure 2. On August 8 (near the time of the strong wind shift passage at Raizet), the wave appears as a region of enhanced convective cloudiness in the shape of an "inverted V" near 60°W and between 15° and 20°N. Such inverted V cloud patterns as indicators of easterly waves have been documented by Frank (1969).

On August 9 (fig. 2b), the increased cloudiness near 70°W and just east of the upper cold Low again coincided with the surface position of the advancing (but weakening) wave. A significant change from August 8 was that the cloud mass extended farther northward and included considerable dense middle and upper layers in addition to the convective towers rooted in the low levels (see surface data of fig. 6). These changes strongly suggest that interaction with the upper cyclone had begun and that the moisture surge associated with the low-level wave was rising to higher levels under the influence of upward vertical motion on the eastern flank of the cold Low. The calculated ω patterns, discussed later, support this view.

The further large increase in cloudiness on August 10 in the vicinity of the cold Low is believed to have been caused by a continuation of the process just described. The calculated ω patterns show widespread upward motion at 700 mb and higher levels. Additional factors may have been (1) the lessened static stability within the cold Low (relative to the environment) that would favor the production of convective cloud and (2) lateral advection of high cloud by the strong upper level winds.

Meanwhile on August 10, the low-level wave as a perturbation in the wind and pressure fields had become unrecognizable in the region 20°–25°N (fig. 3b). Riehl (1965) has stated that a deep easterly current extending to at least 400 mb is needed for the propagation of waves. In the present case, it would appear that the interruption of the easterly current over the Bahamas by the cyclonic circulation existing at and above 500 mb caused the disappearance of the low-level perturbation over that area on August 10. However, the southern portion of the wave, being neither beneath the upper level cyclone nor interrupted by it, continued westward across the Caribbean on August 10 and 11 (figs. 3b, 3c, and 7). Associated dense cloud masses can be seen over the extreme western Caribbean on August 11 (fig. 2d).

STRUCTURE OF COLD LOW ON AUGUST 10 AND 11

Figures 9 and 10 are the vertical cross sections for 1200

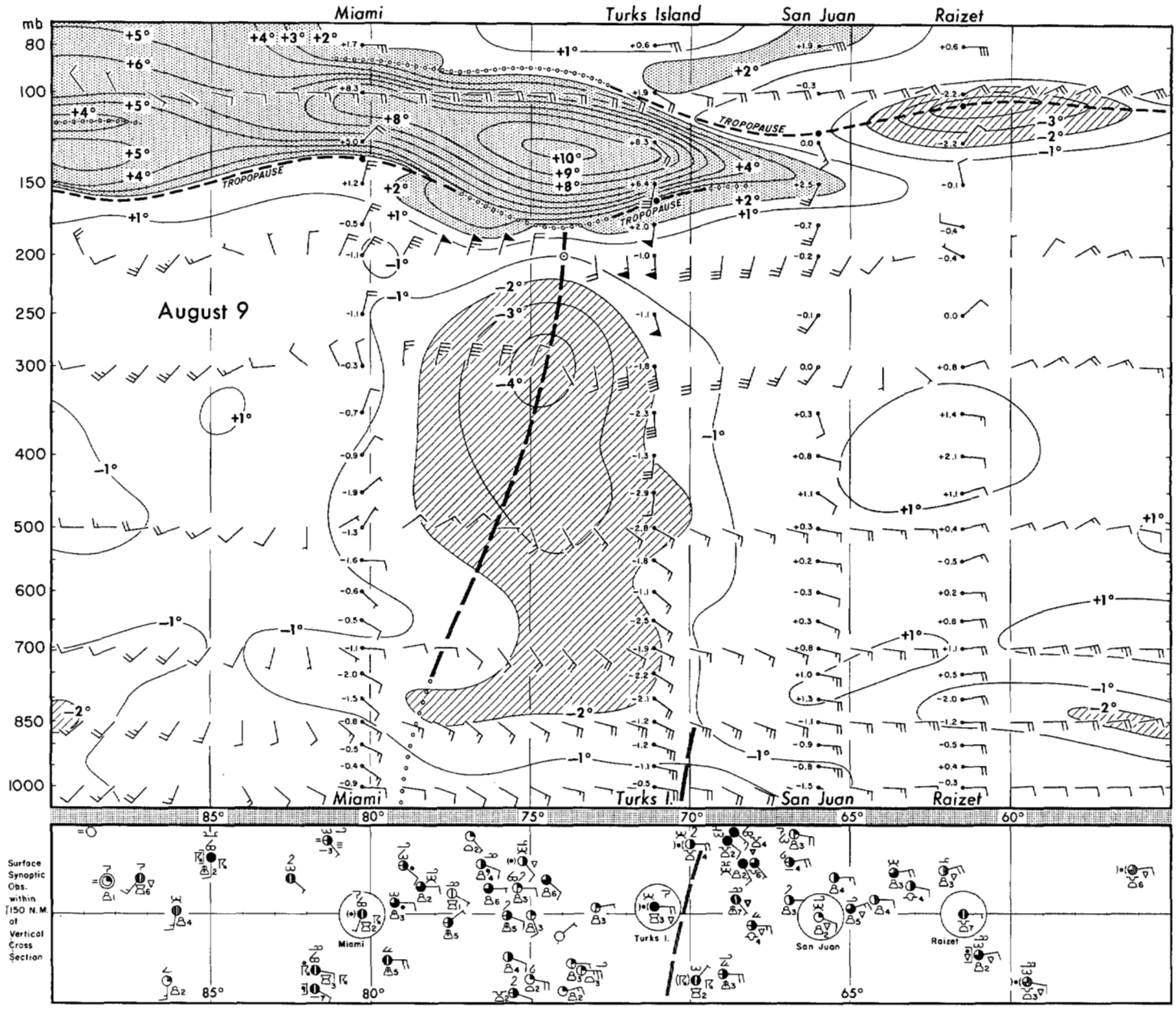

FIGURE 6.—Vertical cross section for 1200 GMT on August 9 along the line shown on figure 1. The isolines are temperature deviations (°C) from the mean Caribbean atmosphere for August (Jordan 1957), based on smoothed analyses (plotted temperatures are unsmoothed). The shaded areas represent deviations exceeding 2°C. The intermediate winds are from streamline-isotach analyses. All winds are plotted in the standard synoptic convention (full barb=10 kt, wind from left to right is from the west, top to bottom is north, etc.). The heavy dashed lines near 75° and 70°W are axes of the upper level cyclonic curvature and the low-level wave, respectively.

GMT on August 10 and 11, respectively. By comparison with August 9 (fig. 6), it is seen that the upper Low had weakened considerably by August 11 and temperature anomalies had become much less pronounced. The primary tropopause over Miami and nearby stations was reforming near 100–110 mb.

5. DIAGNOSTIC RESULTS OF VERTICAL MOTION

Numerical analyses of six forcing functions contributing to vertical motion (ω) as well as the patterns of total ω were obtained for 300, 500, 700, and 900 mb for August 9, 10, and 11. The six forcing functions are identified in table 1. The model has been described in detail by Krishnamurti (1968). Its application to another case study in the Tropics has been reported by Baumhefner (1968).

General results obtained with the individual forcing functions in the present study are given in condensed form in table 2. Figures 11 and 12 show a few of the distributions of calculated values. These include for all days the patterns of total ω at 700 and 300 mb and for August 9

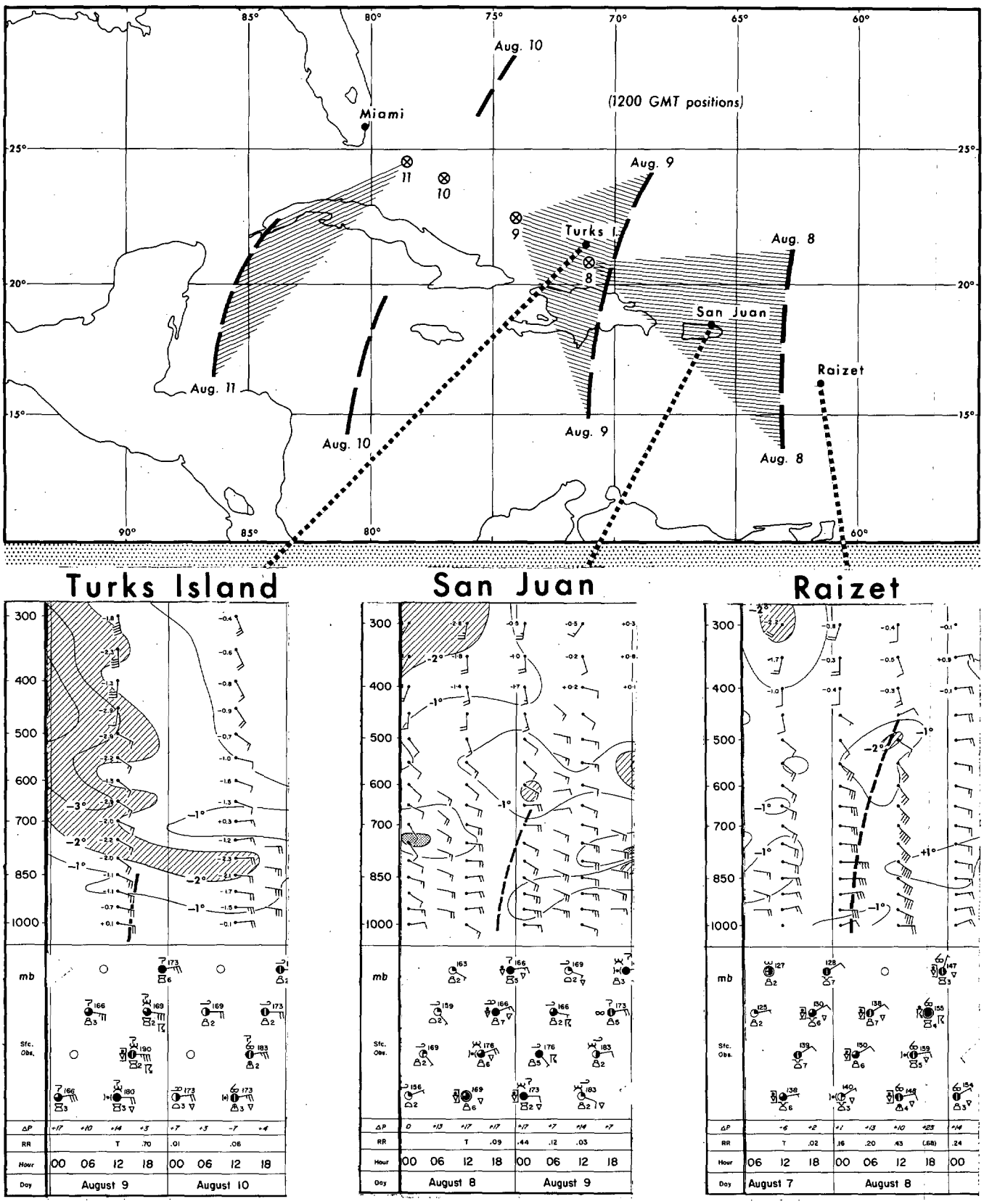

FIGURE 7.—(Upper) the separation distances (shaded areas) between the 200-mb Low center (cross within a circle) and the advancing low-level wave (heavy dashed lines) on Aug. 8–11, 1966, at 1200 GMT; (lower) the vertical time sections for Raizet, Guadeloupe, San Juan, Puerto Rico, and Turks Island showing the passage of the low-level wave at those stations. The isolines are temperature deviations (°C) from the mean Caribbean atmosphere for August (Jordan 1957). The ΔP is the 24-hr sea-level pressure tendency (to 0.1 mb) for the period ending at the indicated hour. RR is the 6-hr rainfall amount (to 0.01 in.).

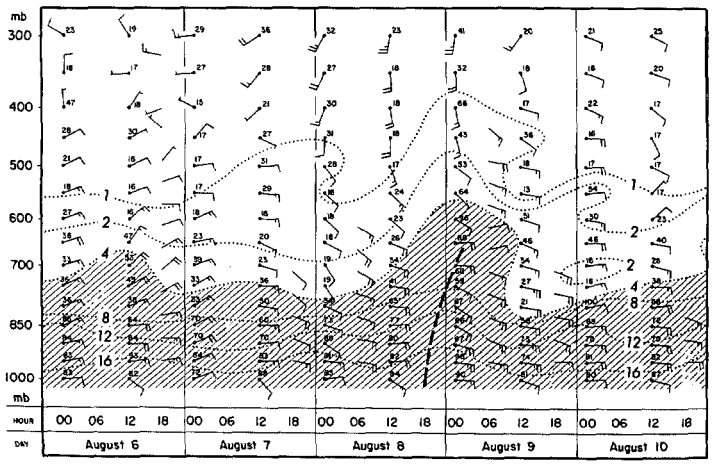

FIGURE 8.—Moisture analysis for San Juan, Puerto Rico, on Aug. 6–10, 1966. The isolines show the mixing ratio (g kg^{-1}). The plotted numbers show the relative humidity (percent).

the thermal contributions at those levels. A few representative vertical profiles of ω for August 9 appear in figure 13.

The main points of interest are:

1. Good agreement between areas of major cloudiness (fig. 2) and areas of upward total ω (figs. 11 and 12). In particular, the area of dense convective and cirriform clouds near 70°W on August 9 agrees well with the upward motion at 300 mb in that locale. The more widespread cloudiness over the Bahamas on August 10 also agrees fairly well with the general upward motion on that day. However, the calculated ω values, overall, are relatively small (the maximum values at 300 mb are on the order of 100×10^{-5} mb s^{-1}—roughly equivalent to 2 cm s^{-1}).

2. Relative dominance of the thermal term, especially at upper levels. This is seen by a comparison of the 300-

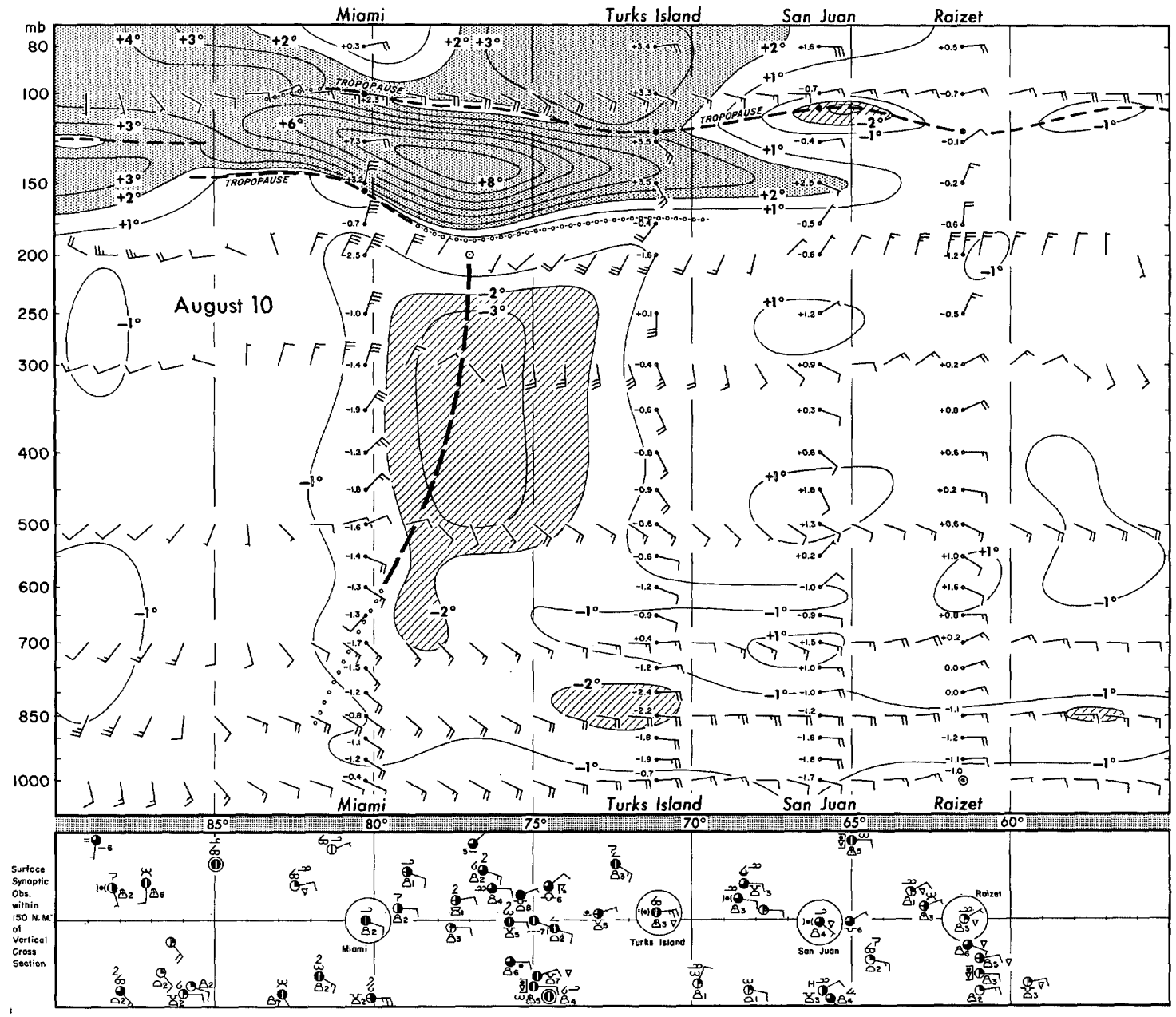

FIGURE 9.—Vertical cross section for 1200 GMT on August 10 (see the caption of fig. 6 for details).

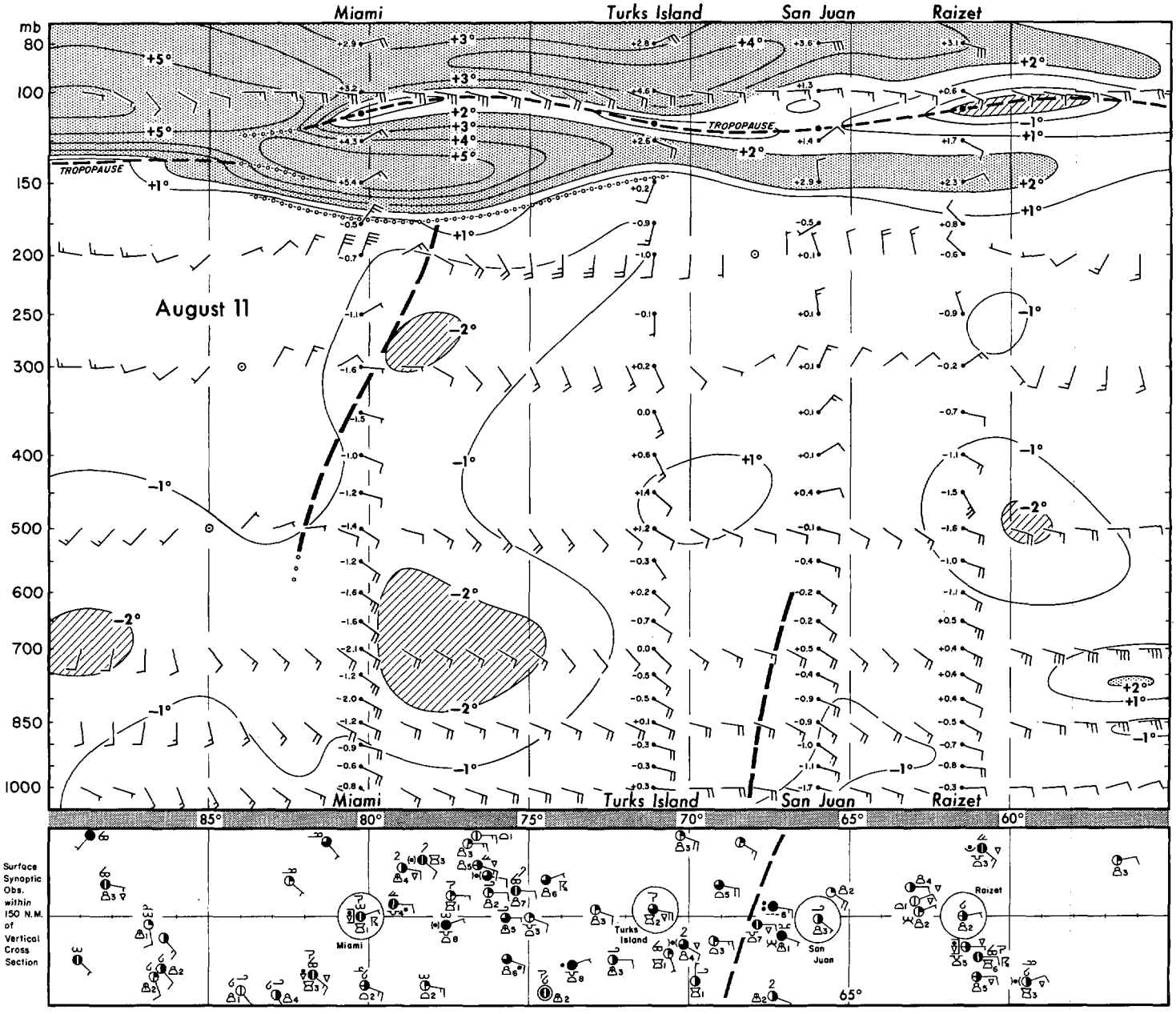

FIGURE 10.—Vertical cross section for 1200 GMT on August 11 (see the caption of fig. 6 for details).

mb total ω pattern in figure 11a with that of the 300-mb thermal component (fig. 11b). Those two patterns are strikingly similar. Vertical profiles near the periphery of the upper level cyclone (fig. 13) also show the thermal term to be overpowering at high levels. Its overall relative importance (percentage contributions of table 2) is less pronounced but still dominant.

3. Importance of the vorticity and deformation terms—less than the thermal contribution but considerably more than the others, except friction at lower levels (table 2).

4. Importance of friction at the lowest (900-mb) level (see table 2).

5. Overall, the tendency toward mostly upward motion east and southeast of the 200-mb Low and mostly downward motion to the west and northwest of it (figs. 11–13).

6. DISCUSSION OF RESULTS

The existence of relatively pronounced calculated upward motion in the dense-cloud area, 70°W, 20°–25°N, on August 9 is significant. It supports the view that an interaction between the upper level cyclone and an approaching low-level wave was occurring in that area at that time. Because this upward motion was mainly at middle and upper levels and was largely due to the thermal forcing function, the upward motion must be regarded as mainly tied to the cold Low itself rather than to the approaching wave. On the other hand, the moisture influx was clearly associated with the approaching low-level wave. The interaction, then, was a coupling between upward motion (mostly at middle and upper levels)

acting on the influx of moisture (mostly at lower and middle levels but with considerable extension into the field of upward motion). On a smaller scale, the embedded convective cores, pumping moisture rapidly upward from low to high levels, undoubtedly contributed to the moisture increase at middle and upper levels. The overall result was the dense and expanding shield of multilayer and convective cloudiness seen on August 9.

The situation on the previous day, August 8, strongly suggests that neither the upward motion alone nor the moisture surge alone would have been sufficient to produce such a cloud mass. On August 8, the vigorous wave and moisture surge, then over the Lesser Antilles, was associated mainly with low-based convective cloudiness. The equally vigorous cold Low, several hundred miles to the west-northwest, contained almost no cloudiness.

Frank (1969) has noted the tendency for cloud enhancement or "blowups" in the area immediately east or southeast of a 200-mb trough or Low in the Tropics. The present case (on August 9) would seem to be an excellent example. The linkage between low-level wave and upper level Low, which was the primary cause of cloud enhancement in the present case, is believed to be a likely cause of other cases of cloud blowup. The area east and southeast

TABLE 1.—*Chief forcing functions of the general balance ω equation (from Krishnamurti 1968)*

1. $f\frac{\partial}{\partial p}J(\psi, \zeta_a)$	Differential vorticity advection by the nondivergent part of the wind
2. $\pi\nabla^2 J(\psi, \theta)$	Laplacian of thermal advection by the nondivergent part of the wind
3. $-2\frac{\partial}{\partial t}\frac{\partial}{\partial p}J\left(\frac{\partial\psi}{\partial x}, \frac{\partial\psi}{\partial y}\right)$	Differential deformation effect
4. $-f\frac{\partial}{\partial p}(\zeta\nabla^2\chi)$	Differential divergence effects
5. $f\frac{\partial}{\partial p}g\frac{\partial}{\partial p}\left[\frac{\partial\tau_y}{\partial x}-\frac{\partial\tau_x}{\partial y}\right]$	Effect of frictional stresses
6. $-\frac{R}{c_p p}\nabla^2 H_L$	Effect of latent heat

TABLE 2.—*Percentage contributions to vertical motion over a 121-grid-point area (approximately 16°×16°) centered at the upper level cyclone. The percentages are based on absolute values. The largest contribution at each individual level is italicized (see table 1 for definition of functions).*

Forcing function	August 9				August 10				August 11				3-day avg.
	300	500	700	900	300	500	700	900	300	500	700	900	
	(mb)				(mb)				(mb)				
1. Vort.	19	36	*42*	27	24	21	32	22	31	17	26	21	27
2. Thermal	*50*	*37*	34	*33*	*46*	*48*	*43*	*44*	*47*	*61*	*51*	*49*	45
3. Def.	27	20	9	8	25	23	10	8	14	7	7	6	14
4. Div.	2	1	2	4	3	2	2	3	4	2	2	5	3
5. Friction	2	5	12	27	2	6	12	23	2	9	12	18	11
6. LH	0	1	1	0	0	1	1	0	1	5	3	1	1

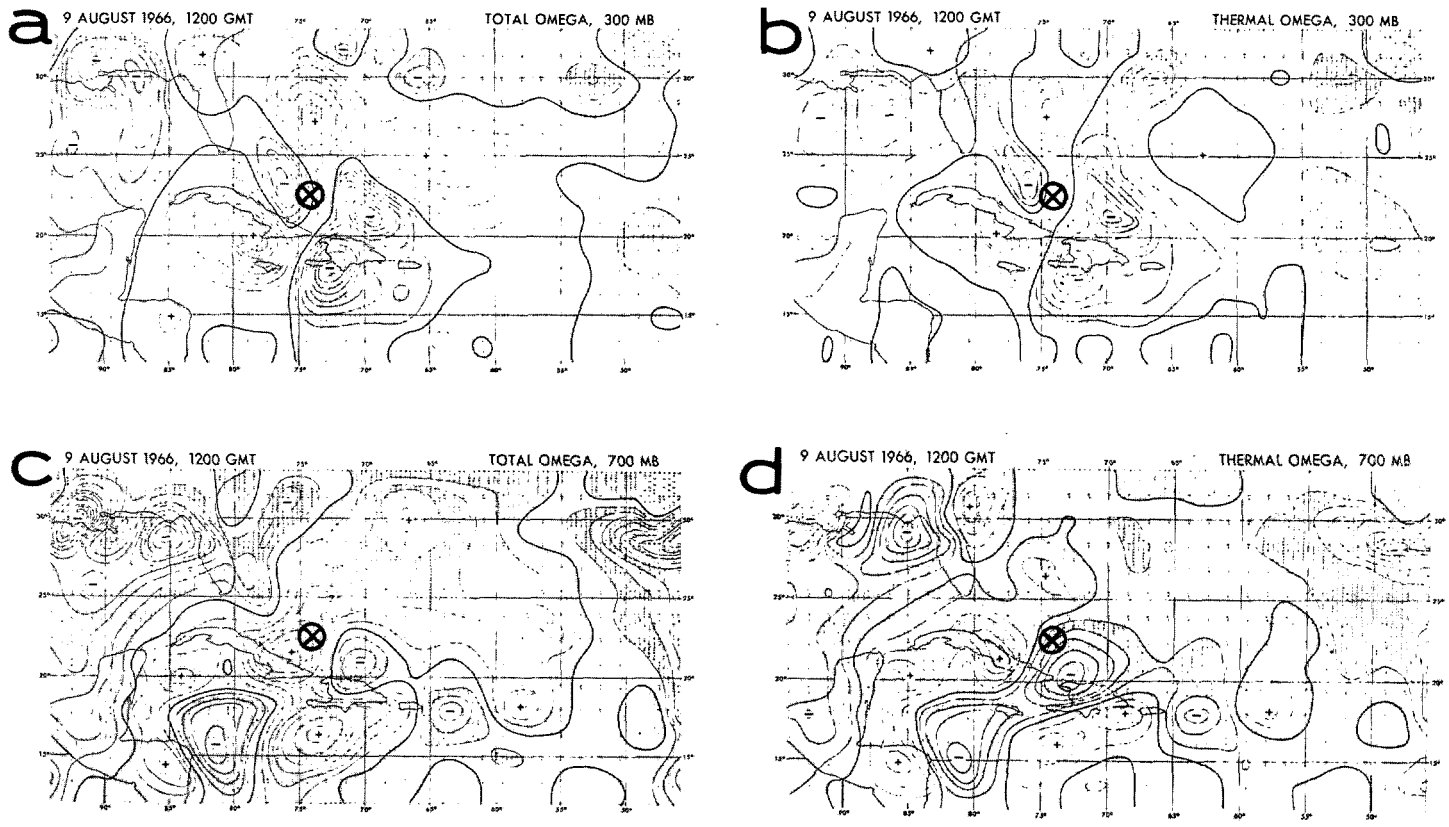

FIGURE 11.—Total ω at 300 mb (a) and 700 mb (c) for 1200 GMT on August 9 and the contribution of the thermal term at those levels (b, d). The isoline interval is 10×10^{-5} mb s^{-1}. The centers of upward and downward motion are indicated by the minus and plus signs, respectively. The position of the 200-mb Low center is indicated by a cross within a circle.

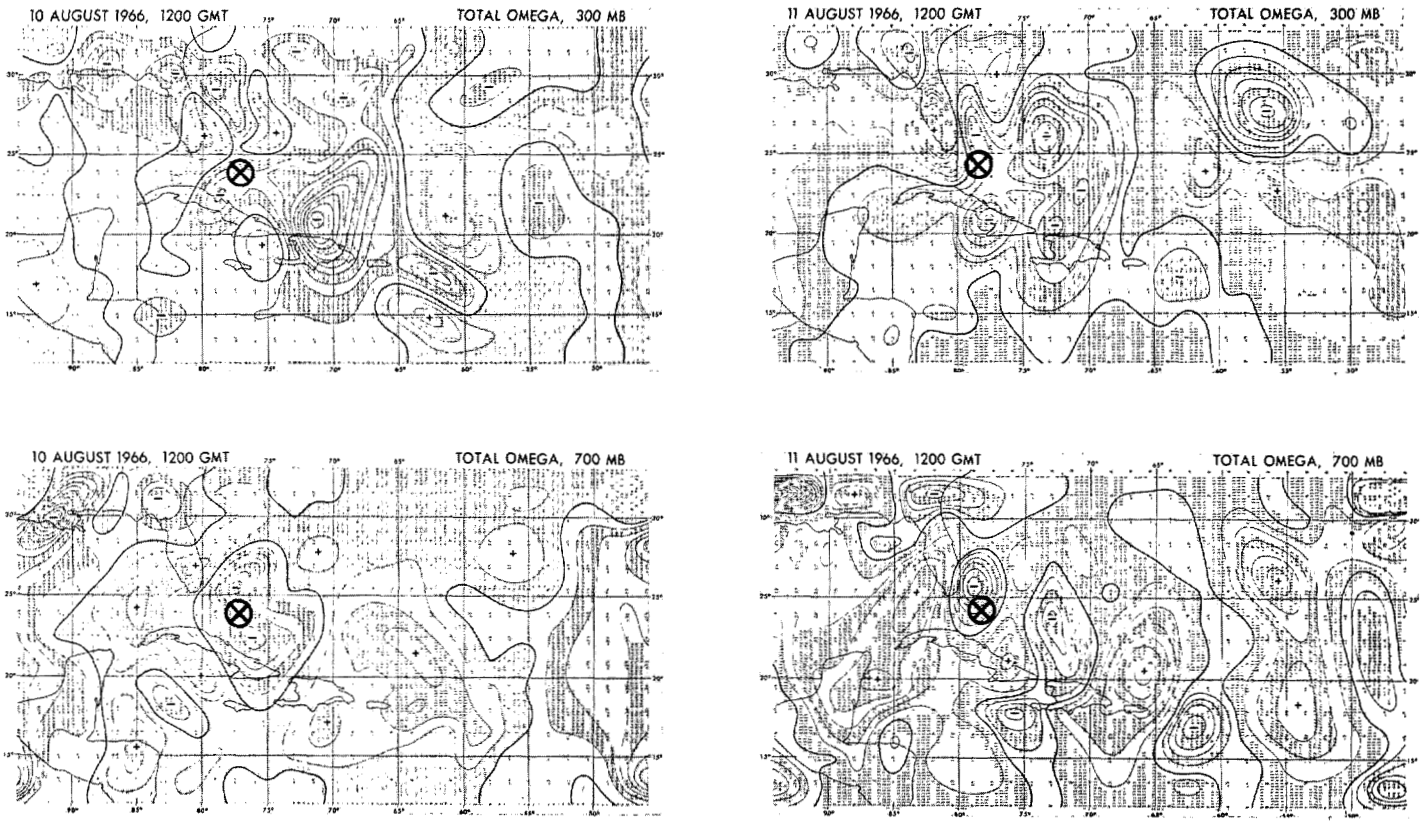

FIGURE 12.—Total ω at 300 and 700 mb for 1200 GMT on August 10 and 11 (see the caption of fig. 11 for details).

of the upper Low would be favored because the more rapidly moving low-level waves would tend to approach the upper Low from that direction.

The existence of tropopauses at more than one level over certain areas, as shown in figures 6, 9, and 10, is a feature that was noted some years ago by Graves (1951) in a study of tropopause heights above San Juan, Puerto Rico. The cross sections of the present study were prepared while the author was unaware of Graves' work; however, they do support his concept of primary and secondary tropopause levels. Graves also noted the tendency for minimum temperature anomalies (cold Lows) to occur at and below minimum secondary tropopause elevations. This likewise was true of the cold Low of the present study; although on August 9, both the primary and the secondary tropopauses in the area directly above the Low were so weak as to be almost nonexistent.

Some other findings of this study also corroborate the work of other investigators. In particular, the relative importance of thermal and vorticity contributions to ω and the small maximum values of ω were observed by Baumhefner (1968) and by Krishnamurti and Baumhefner (1966). Because the numerical models employed and the disturbances studied were not greatly different, these similarities perhaps are to be expected. In all three cases, there has been gross agreement between areas of cloudiness and areas of numerically calculated upward motion, lending support to the general validity of the models. The small (by mid-latitude standards) maximum values of ω of 1 to 2 cm s^{-1} in the present case probably are not unrealistic for synoptic scale tropical disturbances.

The deep upper tropospheric cold Low of the present case may have been associated with upper level vertical motions even more complicated than those numerically determined. Certainly, the vertical arrangement of temperature anomalies in figure 6 together with the coincident destruction of the tropopause suggests a pattern of upward motion and adiabatic cooling in the middle troposphere, subsidence and warming in the lower stratosphere, and near-zero vertical motion (with considerable net horizontal divergence) at some in-between level near 200 mb. But this numerical model assumes zero vertical motion at 100 mb and a smooth interpolation between 100 and 300 mb, giving ω the same sign throughout the depth of that layer. Thus the model, while adequate for lower levels, probably lacked sufficient vertical resolution above 300 mb for this particular situation.

With respect to the importance of the thermal contribution to vertical motion, one might argue that the well-developed cold Low of this study represents a stronger than usual thermal system. However, with the tropical atmosphere as poorly observed as it is and cold Lows already known to be prevalent, there is reason to suspect that temperature gradients of the magnitude of this case may be more common than previously supposed. It is perhaps significant that studies emphasizing thermal effects (e.g., Baumhefner 1968 and Krishnamurti and Baumhefner 1966) are relatively few and recent. Continuing experiments with tropical numerical models and the addition of data from new atmospheric sensors such as the Satellite Infrared Spectrometer may help to determine the true importance of thermal gradients in the Tropics.

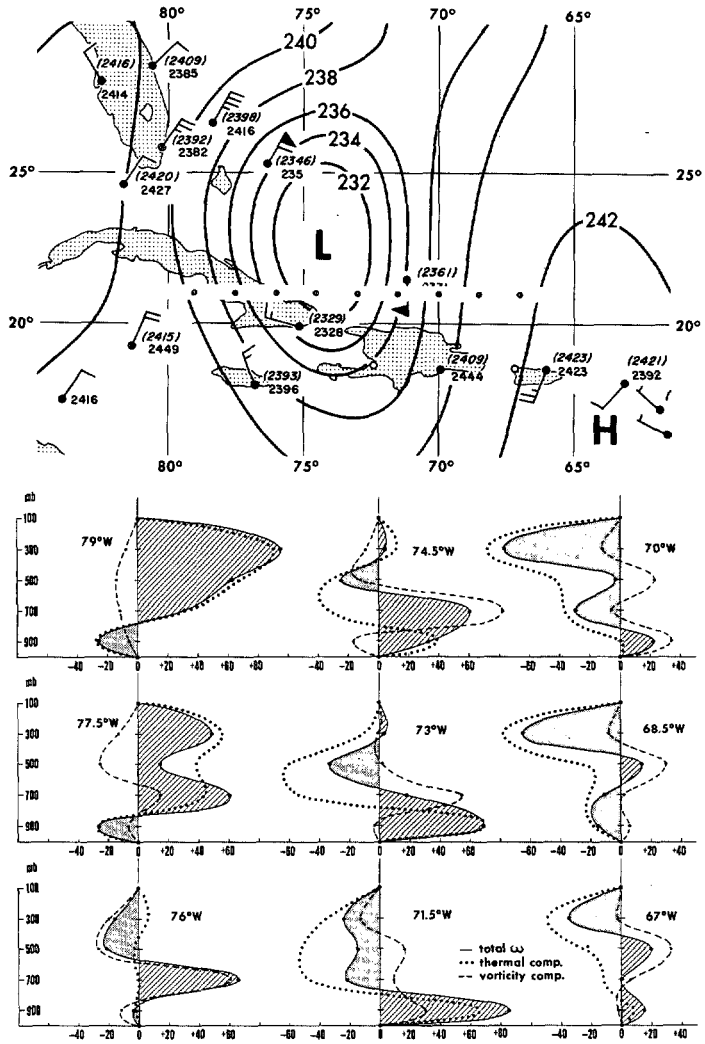

FIGURE 13.—(Upper) the 200-mb analysis for 1200 GMT on August 9; small dots mark the locations of the profiles shown in the lower portion of the figure; (lower) the vertical profiles of total ω (shaded areas) and the contributions from the thermal and vorticity terms at points along latitude 21°N for 1200 GMT on August 9 (abscissa units, 10^5 mb s^{-1}).

7. CONCLUSIONS

The cold Low of this case was a significant thermal system with large temperature anomalies in both the upper troposphere and lower stratosphere. Such systems probably are common in the Tropics.

The chief conclusions are:

1. The cloudiness and weather increased due to temporary linkage between the upper level cyclone and the approaching low-level wave. Much of the upward motion was induced by the upper level cyclone and its thermal configuration. The low-level wave provided the moisture influx.

2. The Laplacian of thermal advection was the single most important forcing function in the pattern of vertical motion. Vorticity and deformation terms also were important.

3. The overall pattern of numerically computed vertical motion showed good agreement with the satellite-observed cloud pattern.

Conclusions (1) and (2) may well apply to a substantial degree in other tropical weather situations. To that extent, they have forecasting implications. Had several features of this complicated situation (cloud photos, numerical diagnoses, moisture distribution) been simultaneously available in real time, it would seem that the combination would have had considerable forecasting value.

ACKNOWLEDGMENTS

The numerical analyses were obtained through the kind cooperation of Prof. T. N. Krishnamurti who designed the model and arranged for the computer facilities at the Florida State University. For helpful discussions and advice, I am also indebted to Prof. Krishnamurti as well as to my colleagues, Mr. Lester F. Hubert and Drs. Christopher Hayden and Jay Winston.

Much of the drafting of the figures was done by Mr. Leonard Hatton.

REFERENCES

Baumhefner, David P., "Application of a Diagnostic Numerical Model to the Tropical Atmosphere," *Monthly Weather Review*, Vol. 96, No. 4, Apr. **1968**, pp. 218–228.

Carlson, Toby N., "Project ECCRO: A Synoptic Experiment in the Tropics," *ESSA Technical Memorandum* IERTM-NHRL 80, U.S. Department of Commerce, National Hurricane Research Laboratory, Miami, Fla., Aug. **1967**, 31 pp.

Frank, Neil L., "The 'Inverted V' Cloud Pattern—An Easterly Wave?," *Monthly Weather Review*, Vol. 97, No. 2, Feb. **1969**, pp. 130–140.

Graves, Maurice E., "The Relation Between the Tropopause and Convective Activity in the Subtropics (Puerto Rico)," *Bulletin of the American Meteorological Society*, Vol. 32, No. 2, Feb. **1951**, pp. 54–60.

Hawson, C. L., and Caton, P. G. F., "A Synoptic Method for the International Comparison of Geopotential Observations," *Meteorological Magazine*, Vol. 90, No. 1073, Dec. **1961**, pp. 336–344.

Jordan, Charles L., "A Mean Atmosphere for the West Indies Area," *National Hurricane Research Project Report* No. 6, U.S. Weather Bureau, Washington, D.C., May **1957**, 17 pp.

Krishnamurti, T. N., "A Diagnostic Balance Model for Studies of Weather Systems of Low and High Latitudes, Rossby Number Less Than 1," *Monthly Weather Review*, Vol. 96, No. 4, Apr. **1968**, pp. 197–207.

Krishnamurti, T. N., and Baumhefner, David P., "Structure of a Tropical Disturbance Based on Solutions of a Multilevel Baroclinic Model," *Journal of Applied Meteorology*, Vol. 5, No. 4, Aug. **1966**, pp. 396–406.

Riehl, Herbert, *Tropical Meteorology*, McGraw-Hill Book Company, Inc., New York, **1954**, 392 pp.

Riehl, Herbert, "Comments on Waves in the Easterlies," *Journal of Applied Meteorology*, Vol. 4, No. 1, Feb. **1965**, pp. 149–150.

Simpson, Joanne, Garstang, Michael, Zipser, Edward J., and Dean, Gordon A., "A Study of a Non-Deepening Tropical Disturbance," *Journal of Applied Meteorology*, Vol. 6, No. 2, Apr. **1967**, pp. 237–254.

[*Received September 15, 1969; revised May 14, 1970*]